Available online at www.sciencedirect.com
ScienceDirect
Metabolic Engineering 9 (2007) 419–432
METABOLIC ENGINEERING
www.elsevier.com/locate/ymben

A metabolic flux analysis to study the role of sucrose synthase in the regulation of the carbon partitioning in central metabolism in maize root tips ☆

Ana Paula Alonso[a], Philippe Raymond[a], Michel Hernould[a], Corinne Rondeau-Mouro[b], Albert de Graaf[c], Prem Chourey[d], Marc Lahaye[b], Yair Shachar-Hill[e], Dominique Rolin[a], Martine Dieuaide-Noubhani[a,*]

[a]*INRA, Université Bordeaux 1, Université Victor Segalen Bordeaux 2, UMR 619 Biologie du fruit, BP 81, 33883 Villenave d'Ornon cedex, France*
[b]*INRA, UR 1268 Biopolymères, Interactions, Assemblages, BP 71627, 44316 Nantes cedex 03, France*
[c]*Department of Surgery, Maastricht University, P.O. Box 616, 6200 MD Maastricht, The Netherlands*
[d]*United States Department of Agriculture, Agricultural Research Service & University of Florida, Gainesville, FL 32611-0680, USA*
[e]*Department of Plant Biology, Michigan State University, East Lansing, MI 48824, USA*

Received 22 December 2006; received in revised form 26 June 2007; accepted 26 June 2007
Available online 10 July 2007

Abstract

In order to understand the role of sucrose synthase (SuSy) in carbon partitioning, metabolic fluxes were analyzed in maize root tips of a double mutant of SuSy genes, *sh1 sus1* and the corresponding wild type, W22. [U-^{14}C]-glucose pulse labeling experiments permitted the quantification of unidirectional fluxes into sucrose, starch and cell wall polysaccharides. Isotopic steady-state labeling with [1-^{13}C]-, [2-^{13}C]- or [U-^{13}C]-glucose followed by the quantification by ^{1}H-NMR and ^{13}C-NMR of enrichments in carbohydrates and amino acids was also performed to determine 29 fluxes through central metabolism using computer-aided modeling. As a consequence of the suppression of SUS1 and SH1 isozymes, maize root tips diameter was significantly decreased and respiratory metabolism reduced by 30%. Our result clearly established that, in maize root tips, starch is produced from ADP-Glc synthesized in the plastid and not in the cytosol by sucrose synthase. Unexpectedly, the flux of cell wall synthesis was increased in the double mutant. This observation indicates that, in maize root tips, SH1 and SUS1 are not specific providers for cellulose biosynthesis.

Keywords: Sucrose synthase; Metabolic flux analysis; Cell wall; Maize root; Isotopic labeling; NMR

1. Introduction

In higher plants, sucrose import and metabolism plays an important role in the development of non-photosynthetic tissues. Two classes of enzymes are involved in sucrose breakdown: sucrose synthase (SuSy) activities catalyse the reversible conversion of sucrose to UDP-Glc and fructose, and invertases hydrolyze sucrose to glucose and fructose. UDP-Glc may then be used for cellulose synthesis (Ruan et al., 1997) or converted to Glc-1-P and Glc-6-P via the UDP-Glc pyrophosphorylase and phosphoglucomutase reactions. Free Glc and fructose are further converted to hexose-phosphates (hexose-P) by hexokinase. The hexose-P are either catabolized in the cytosol through the glycolysis and the tricarboxylic acid cycle thus feeding energy for biosynthetic reactions (Xu et al., 1989; Wang et al., 1993; Nolte and Koch, 1993; Zrenner et al., 1995), or are used as substrate for biosynthetic pathways, such as starch or cell wall polysaccharides syntheses.

According to the literature, SuSy could play a role in the regulation of carbon partitioning in plant cells. In many

☆This work was supported by a grant from the Institut National de la Recherche Agronomique (INRA), Université Victor Segalen Bordeaux 2, Université Bordeaux I, the Conseil Régional d'Aquitaine and by a doctoral fellowship from INRA and the Conseil Régional d'Aquitaine.
*Corresponding author. Fax: +33 5 57 12 25 41.
E-mail address: dieuaide@bordeaux.inra.fr (M. Dieuaide-Noubhani).

1096-7176/$ - see front matter © 2007 Elsevier Inc. All rights reserved.
doi:10.1016/j.ymben.2007.06.002

studies, SuSy mutants or down-regulated transgenic plants present decreased starch content, at least in starch storing tissues (Chourey et al., 1998) which may be explained by a decreased supply of hexose-P to plastids in the mutant compared to wild type. However, alternative mechanisms have also been proposed. The decreased level of starch in the endosperm of the *sh1* maize mutant was associated with the degeneration of starch storing cells (Chourey et al., 1998). Alternatively, genetic and biochemical evidences from studies of cereal endosperm suggested that ADP-Glc, the substrate of starch synthase, is synthesized in the cytosol by SuSy and imported to plastids (Shannon et al., 1996; Baroja-Fernandez et al., 2003, 2004). Whether this is limited to the endosperm of cereals or also occurs in other cell types is presently a matter of debate (Neuhaus et al, 2005). SuSy also would play a preponderant role in cell wall polysaccharides synthesis. It is now assumed that a non-soluble form of SuSy would address UDP-Glc directly for cellulose synthesis. In this model, the free pool of UDP-Glc would not participate in cellulose synthesis, or only in an indirect way, by increasing the synthesis of sucrose (Haigler et al., 2001).

In maize, SuSy is encoded by three non-allelic genes now called *Sh1* (“Shrunken”), *Sus1* (Chourey, 1981) and *Sus2* which encode the SH1, SUS1 and SUS2 isozymes, respectively (Chourey, 2006). The *Sh1* gene is highly expressed in developing endosperm while *Sus1* and *Sus2* (Chourey et al., 1986; Carlson et al., 2002) are expressed in almost all tissues, being abundant in root, etiolated shoot and kernel, and nearly absent from the green shoot, ovules and mature pollen. The *sh1* mutant bearing a deletion of the *Sh1* gene, presents the “shrunken” phenotype with a decreased level of starch in seed, which was related with the degeneration of endosperm cells. A comparison between the *sus1-1* mutant with decreased expression of the SUS1 protein (then named SS1) and the double mutant *sh1 sus1-1* (referred to hereafter as W22dm) (Chourey et al., 1998), the latter with similar cellular degeneration but lower starch content than the *sh1* mutant, suggested that SH1 plays the preponderant role in supplying UDP-Glc for cellulose synthesis whereas SUS1 generates precursors for starch synthesis. SUS2 accounts for the residual, 0.5% of wild type (W22wt), SuSy activity in the W22dm endosperm. Its role is not established (Carlson et al., 2002). It must be noted that in the absence of direct measurements of the fluxes of starch and cell wall synthesis and degradation, interpretations of the effects of SuSy deletion on cell metabolism remain speculative.

SuSy catalyzes a near equilibrium reaction (Geigenberger and Stitt, 1993) which, together with UDP-Glc pyrophosphorylase and hexose-P isomerase, maintains rapid near equilibrium interconversions between the large sucrose, UDP-Glc and Hexose-P pools, which is important in providing abundant substrates for the numerous pathways that are connected to these pools, thus contributing to the robustness of plant cell metabolism (Rontein et al., 2002).

The aim of the present work was to evaluate the role of SuSy in the regulation of central metabolism and carbon partitioning in maize root tips by comparing sugar metabolism in W22dm lacking SH1 and SUS1 (Chourey et al., 1998) to that of the W22wt. Metabolic flux analysis was carried out by combining pulse- and steady-state labeling experiments with [1^{14}C]-, [U^{13}C]-, [1^{13}C]- and [2^{13}C]-Glc. Analysis of purified carbohydrates and amino acids (alanine and glutamate) by ^{1}H-NMR and ^{13}C-NMR permitted the quantification of the specific enrichment of their carbon atoms. The fluxes of intermediary metabolism were determined using a computer-aided modeling approach for metabolic pathways. By this way, 33 fluxes in the central metabolism and into structural and storage carbohydrates were quantified. Compared to the wild type, the double mutant for SuSy showed a higher rate of cell wall synthesis, unchanged fluxes through substrate cycles and reduced glycolysis and respiration rates. These observations were corroborated by cytological and biochemical analysis. These results are discussed in relation to the involvement of SuSy in the partitioning of carbon fluxes.

2. Materials and methods

2.1. Materials and incubations

Maize seeds (W22 wild type, noted W22wt or W22 *sh1 sus1*, noted W22dm) were germinated for 3 days in darkness at 25 °C as described by Brouquisse et al. (1991). The 3.5 mm tips of primary roots were excised.

2.1.1. Steady-state labeling experiments

The present labeling experiments were performed simultaneously with those published in Alonso et al. (2005). In ^{13}C labeling experiments, 150–200 excised root tips were incubated for 25 h with 200 mM D-[U-^{13}C]-Glc (99% enrichment) or D-[1-^{13}C]-Glc (99% enrichment) or D-[2-^{13}C]-Glc (99% enrichment) in medium A described by Brouquisse et al. (1991), washed with abundant ice-cold water, re-excised at 3.5 mm and frozen in liquid N_2. The apparently high concentration of Glc, intermediate between the sugar concentration in the phloem (0.5 M; Bret-Harte and Silk, 1994) and that in the root tip cell (about 100 mM), is probably close to that physiologically present around the root cells. Moreover, it has been shown that this concentration is necessary to sustain normal respiration rate of the root tips (Saglio and Pradet, 1980) and to avoid induction of proteolytic activities as a consequence of a sugar starvation (James et al., 1993).

2.1.2. Short-term labeling experiments

Maize root tips (10 roots ml^{-1}) were incubated for 25 h in medium A, supplemented with 200 mM Glc, and bubbled with a N_2/O_2 mixture (50/50, v/v). After incubation, the root tips were washed with abundant water to eliminate exogenous Glc, and then further incubated with 200 mM

D-[U-^{14}C]-Glc (specific radioactivity (SR) varying between 30 and 200 dpm nmole^{-1}) for 5–60 min. Roots were harvested by filtration, washed with ice-cold water and re-excised at 3.5 mm before being frozen in liquid N_2. The re-excision was performed after the labeling to avoid the stress due to the excision.

2.2. Preparation of extracts

2.2.1. Acid extracts of Glc-6-P and UDP-Glc

Water-soluble metabolites, including Glc-6-P and UDP-Glc, were extracted using perchloric acid as described by Brouquisse et al. (2001). After extraction, the extracts were dried.

2.2.2. Ethanolic extraction and fractionation of ethanol-soluble compounds

The extraction of soluble compounds was performed as described by Salon et al. (1988). The extract was resuspended in 1 ml water after evaporation. The extracted metabolites were separated as neutral, acidic and cationic fractions and free sugars (Glc, fructose and sucrose) were purified by HPLC from the neutral fraction (Moing et al., 1994).

2.2.3. Starch extraction

Starch was extracted from the residue of ethanolic extraction and further purified as Glc by HPLC as described by Moing et al. (1994).

2.2.4. Cell wall polysaccharide extraction

They were extracted using a protocol described by Gibeaut and Carpita (1991), and modified according to Alonso et al. (2005).

2.3. Analysis of metabolites

2.3.1. Normalization of the radioactivity labeling results

The Glc concentration in all experiments was 200 mM, but in [1-^{14}C]-Glc labeling experiments, the SR of the external Glc varied between 20 and 150 dpm nmol^{-1}. To allow comparison of data from different experiments, all SR values are given after normalization of the SR of external Glc to 1, i.e. after dividing the specific radioactivities measured by the SR of external Glc in the corresponding experiment.

2.3.2. Determination of the SR of soluble sugars, amino acids, Glc-6-P and UDP-Glc after [U^{14}C]-Glc labeling experiments

SR of soluble sugars, amino acids and UDP-Glc were determined after HPLC purification as described by Alonso et al. (2005). SR of Glc-6-P was determined as described by Alonso et al. (2005) from the perchloric extracts.

2.3.3. Determination of enrichments

NMR analyses were performed at 24 °C with a Bruker Avance 500 spectrometer equipped with a 5-mm cryoprobe optimized for detecting ^{13}C. ^{1}H NMR spectra were obtained at 500.16 MHz with a pulse of 10 μs (corresponding to an angle of 90°) using a recycling time greater than $6T_1$. ^{13}C NMR spectra were obtained at 125.77 MHz with a pulse of 6.7 μs (corresponding to an angle of 90°) using a recycling time greater than $6T_1$. For sucrose and Glc, T_1 was measured with an inversion-recovery sequence and found to be respectively, 1.7 and 2.7 s for ^{1}H carried by the C-1, 0.6 and 1.3 s for ^{13}C1, 10.6 and 1.3 for ^{13}C2, 0.6 and 1.4 for ^{13}C3, 0.6 and 1.2 for ^{13}C4, 0.5 and 1.3 for ^{13}C5 and 0.3 and 0.6 for ^{13}C6. For alanine T_1 was 6.6 for ^{1}H carried by the C3, 3.8 for ^{13}C2 and 1.6 for ^{13}C3. And for glutamate T_1 was 2.5 for ^{1}H carried by the C2, 11.2 for ^{13}C1, 1.7 for ^{13}C2, 1.0 for ^{13}C3, 1.2 for ^{13}C4 and 14.4 for ^{13}C5. Peak assignment was performed according to previous studies (Dieuaide-Noubhani et al., 1995; Rontein et al., 2002) and from spectra of pure compounds.

The absolute ^{13}C enrichments of Glc α and β C1, sucrose glucosyl C1, starch glucosyl C1, alanine C3 and glutamate C2 were determined from ^{1}H NMR and ^{13}C NMR spectra as described by Dieuaide-Noubhani et al. (1995). Alonso et al. (2005) determined a diluting factor for Glc and sucrose to be, respectively, 1.066 and 1.038 in W22wt maize root tips. Using identical protocol, starch diluting factor was estimated to be 1.291 in W22wt maize root tips. For W22dm, diluting factors of Glc, sucrose and starch were determined to be 1.045, 1.036 and 1.345, respectively. These diluting factors were applied to the enrichments determined in [1-^{13}C]-Glc and [2-^{13}C]-Glc labeling experiments in order to correct the measurements (Table 2) using the formula: $E_{\text{corrected}} = (E_{\text{measured}} - 1.1)\text{DF} + 1.1$, where DF is the diluting factor.

2.4. Enzyme assays

Enzymatic activities were measured in extracts obtained from 30 to 50 maize root tips re-excised to 3.5 mm after 25 h incubation (Alonso et al., 2005).

2.4.1. Glc-6-phosphatase (EC 3.1.3.9) activity

Glc-6-phosphatase activity was measured on a crude extract as described in Alonso et al. (2005).

2.4.2. Neutral invertase (EC 3.2.1.26) and SuSy (EC 2.4.1.13) activities

Activities of neutral invertase and total sucrose synthase were successively measured essentially according to Pelleschi et al. (1997). Extract was added to an assay mix containing 0.3 M TEA buffer (pH 7.5), 30 mM $MgSO_4$, 110 mM sucrose, 2.5 mM DTT, 1 mM ATP, 0.4 mM NAD, 2 U ml^{-1} hexokinase, 2 U ml^{-1} Glc-6-P isomerase and 1 U ml^{-1} Glc-6-P dehydrogenase. First neutral invertase activity is measured at 30 °C by monitoring NAD reduction at 340 nm. Second the addition of 0.2 mM

UDP induces at 30 °C an increase of the rate of NAD reduction due to sucrose synthase activity. ADP produced by hexokinase, as a consequence of neutral invertase activity could be used as substrate for SuSy, thus leading to an overestimation of invertase and an underestimation of SuSy. According to the invertase activity measured in the extract, and our experimental procedures, a concentration of ADP ranging between 10 and 30 μM was produced, which is about 10 times lower than the K_m of SuSy for ADP (Baroja-Fernandez et al., 2003).

2.4.3. Acid invertase activity

Acid invertase assays were adapted from Lowell et al. (1989). Extract (25 or 10 μl in a total volume of 25 μl) is added to 35 μl of 0.2 M sodium acetate buffer (pH 4.8) containing 110 mM sucrose, allowing acid invertase activity. After 15 min incubation at 30 °C the reaction is stopped by adding 50 μl of 0.6 M sodium phosphate buffer (pH 7.0) and boiling the extract for 5 min. Once the extract cool down at room temperature, 743 μl 0.3 M TEA buffer (pH 7.5) containing 30 mM $MgSO_4$, 1.3 mM ATP, 0.5 mM NAD, 2.7 U ml^{-1} hexokinase, 2.7 U ml^{-1} Glc-6-P isomerase and 1.3 U ml^{-1} Glc-6-P dehydrogenase is added. The mix is incubated at 30 °C for 30 min and then centrifuged at 14,000 rpm for 3 min. Supernatant OD is measured at 340 nm in order to measure NAD reduction and determine acid invertase activity occurred during the 15 min of incubation.

2.4.4. Glucokinase (EC 2.7.1.2) activity

Glucokinase activity was assayed as described by Bouny and Saglio (1996).

2.5. Rate of respiration

Ten maize root tips were transferred to 1.5 ml incubation medium previously bubbled with O_2/N_2 mixture (1:1, v/v). O_2 consumption was measured at 25 °C using a O_2 Clark' electrode (Model 1302; Strathkelvin Instruments, Glasgow, Scotland) connected to an O_2 analyzer (Chemical microsensor 1201; Diamond General Corp., Ann Arbor, MI, USA).

2.6. Histological analysis

Tissues were fixed, embedded in paraffin wax, sectioned and stained as described by Bereterbide et al. (2002).

2.7. Cell wall polysaccharides analysis

Analysis were performed on maize root tips incubated 25 h with [U-^{13}C]-Glc on residues obtained after ethanolic and starch extraction. NMR experiments were performed on maize roots residues dried and rehydrated to saturation with D_2O using a Bruker DMX-400 spectrometer operating at a proton frequency of 400.13 MHz and a ^{13}C frequency of 100.62 MHz. The MAS rate was fixed at 8000 Hz and each experiment was recorded at ambient temperature (293 ± 1 K). The cross-polarisation experiments (CP-MAS) were carried out using a 90° proton pulse around 3.5 μs, a 1 ms contact time at 71 kHz and an acquisition time of 17 ms during which dipolar decoupling (TPPM) of 71 kHz was applied. A typical number of 256 scans were acquired for each spectrum with a recycle time of 5 s. The chemical shifts were determined by using the carbonyl peak of glycine as external reference.

Neutral sugars and uronic acids were quantified in the cell walls of material recovered from CP-MAS ^{13}C NMR experiments. Prior to analysis, the samples were freeze-dried and then for 2 h at 40 °C in vacuum. Neutral sugars were determined according to Englyst and Cummings (1988). Samples were pre-hydrolyzed for 30 min at 25 °C in 26 N sulfuric acid and then for 2 h at 100 °C in 2 N sulfuric acid. Monomers were reduced to alditols by alkaline sodium borohydride and converted to acetates by acetic anhydride and *N*-methylimidazol (Blakeney et al., 1983). They were identified and quantified by gas–liquid chromatography on a BP 225 capillary column (SGE, France SARL; temperature: 205 °C, carrier gas: H_2). For calibration, a standard sugar solution and inositol (the internal standard) were used. Uronic acids in acid hydrolysates were quantified using the metahydroxydiphenyl colorimetric method (Thibault, 1979).

2.8. Flux measurements

2.8.1. Short time labeling method

The unidirectional rate of synthesis of a cellular compound can be measured after short time labeling, by dividing the rate of radioactivity incorporated by the SR of the precursor. The rate of Glc consumption (V_g) was determined by dividing the slope of the curve of radioactivity incorporation by the roots (Fig. 2A) by the SR of extra-cellular Glc. The quantities of radioactivity incorporated into glucosyl moieties of sucrose and starch and into polysaccharides during a time interval were converted to the amount of sugar produced, expressed in mol g FW^{-1}, using the equation:

$$N_{n+1} = N_n + (RA_{n+1} - RA_n)/G6P_n,$$

where N_n, RA_n and $G6P_n$ correspond, respectively, to the number of moles, the radioactivity incorporated into the compound studied (expressed in dpm g^{-1} FW^{-1}), and the SR of Glc 6-P; *n* indicating the *n*th time point (see Alonso et al., 2005). The slope of the curves thus obtained were used to calculate the rate of sucrose, starch and cell wall polysaccharide biosynthesis.

2.8.2. Steady-state labeling method

Flux quantification was made using the software package 13C-FLUX obtained from Dr. W. Wiechert (Department of Simulation, University of Siegen, Germany). The metabolic model depicted in Fig. 1 was programmed in the 13C-FLUX format (Wiechert et al.,

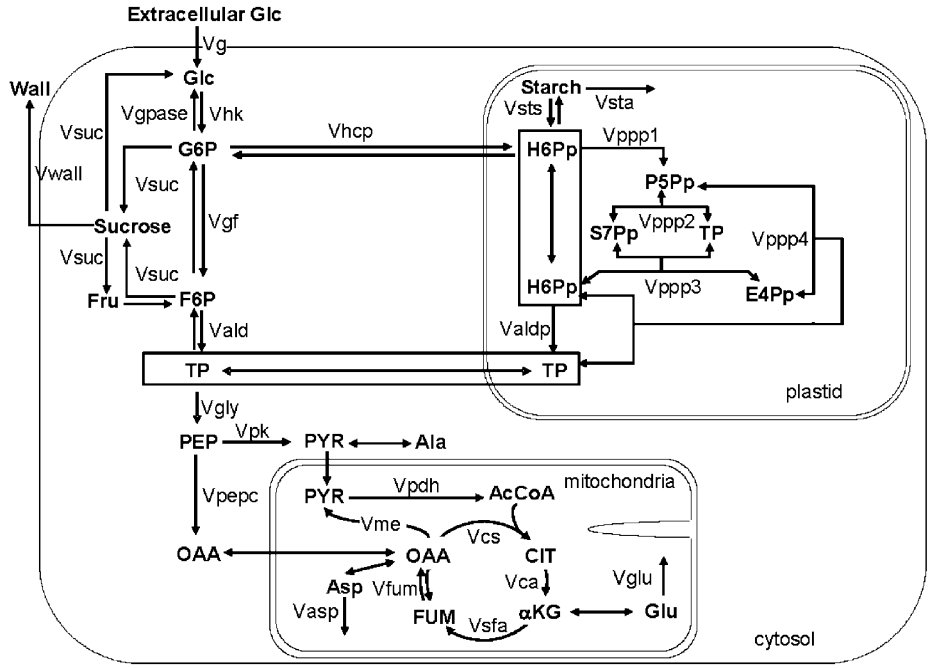

Fig. 1. The network of carbohydrate metabolism in maize root tips. Metabolic pathways have been identified by using the labeling of intermediates as described in the text. Flux abbreviations are described Table 3.

2001) (model available from the authors upon request). In order to include data from the two separate experiments with [1-^{13}C] and [2-^{13}C]-Glc into a single flux estimation procedure, each flux and metabolite pool was in fact programmed doubly (using subscript 1 for the [1-^{13}C]-Glc experiment, and 2 for the [2-^{13}C]-Glc experiment). Equality of identical fluxes in the two separate metabolic networks thus defined was forced by using equality equations, a very convenient feature offered by 13C-FLUX (as an example, $V_{g1}-V_{g2}=0$ is used to equate the Glc uptake rates in both experiments). The following net fluxes V_{res}, V_{aldp}, V_{pppp1}, V_{me}, V_{Co_2} and V_{wall} were set free, whereas V_{sta} was constrained to 0 because there was no net synthesis of starch in maize root tips. The exchange fluxes named V_{gf}, V_{ald}, V_{hcp}, V_{sts}, V_{ppp2}, V_{ppp3}, V_{ppp4} and V_{fum2} were set free, whereas V_{hk}, V_{res}, V_{gly}, V_{aldp}, V_{ppp1}, V_{pk}, V_{pdh}, V_{cs}, V_{ca}, V_{sfa}, V_{me} and V_{pepc} were constrained to 0. The flux values quantified by pulse labeling experiments (V_{suc}, V_{wall} and V_{sts}) as well as V_{res} calculated according to Alonso et al. (2005) were included in the 13C-FLUX model and set as free. The optimization program used was Donlp2 with about 500 different starting points. The best fit that was also the most commonly optimized values for the fluxes is presented Table 3.

3. Results

3.1. Metabolic and isotopic steady state

In W22dm maize root tips incubated with 200 mM [1-^{14}C]-Glc, isotopic steady state was reached within 20 h, as it was in the W22wt root tips, as indicated by the constant specific radioactivities of glutamate and aspartate between 20 and 25 h. In W22wt, the isotopic steady state of starch and the hexose-P was examined further by incubating root tips for 30 h with [1-^{13}C]-Glc. The enrichments of individual carbons in Glc, sucrose, alanine and glutamate were identical to those measured after 25 h. In contrast, the enrichments of starch C-1 and C-6 were increased by 15% (data not shown), but no additional label randomization between C-1 and C-6 was observed. The constant labeling pattern in sucrose and starch strongly suggests that the cytosolic and plastidic hexose-P were already labeled to steady state after 25 h. The increased accumulation of label in starch may be explained in two ways. First, the enrichment of metabolically active starch increases by 15%: the constant labeling pattern of the other carbohydrate pools would indicate that the flux from starch is small, as was already observed in W22wt (Alonso et al, 2005) (see below, for W22dm). This would correspond to a near-steady-state situation. Alternatively, the increased label accumulation in starch may be related with the replacement of the most mature cells, which contain metabolically inactive, unlabeled, starch in the core of starch granules, by newly formed cells that synthesize fully labeled starch grains. Since the starch pool was smaller in W22dm than in W22wt and the rate of starch synthesis (see below) was similar, starch steady state is expected to be reached more rapidly in W22dm than in W22wt. This would correspond to a steady-state situation where the hexose-P produced from starch turnover and those incorporated into starch have the same enrichment, as indicated in the model (Fig. 1). Metabolic steady state was also reached within 15 h as indicated by the stabilization of

the respiratory rate (data not shown). Therefore, the time used for labeling was set to 25 h of incubation after excision of the root tips, for W22dm (present data) as it was for W22wt (Alonso et al., 2005).

3.2. Physiological and biochemical comparison of W22dm and W22wt

After 25 h of incubation, root length was not significantly different but fresh weight was 29% lower in W22dm than in W22wt root tips (Table 1) according to the fact that the root diameter is smaller in the double mutant.

Additional physiological and biochemical studies were performed after excising the roots to a length of 3.5 mm (Table 1). Oxygen uptake rate was 28% lower in W22dm than in W22wt root tips. Glc and sucrose contents were not significantly different on a FW basis while fructose and starch contents were lower by, respectively, 33% and 69% in W22dm. The levels of UDP-Glc and Glc-6-P pools were not affected by the reduction of SuSy activity. Similarly, Shannon et al. (1996) reported no differences in the levels of UDP-Glc between the W22wt and W22dm developing endosperm which retains less than 5% of the WT levels of SuSy activity. Enzyme activities involved in sucrose metabolism and Glc-6-P cycling were also measured (Table 1). W22dm had about 5% of wild type SuSy activity. Acid invertase was about 12 times more active than neutral invertase in W22wt and was significantly lower in W22dm. Glucokinase and Glc-6-phosphatase activities, measured at pH 7.5, were not significantly different in W22wt and W22dm root tips.

Table 1
Physiological and biochemical characterization of W22wt and W22dm root tips

	W22wt	W22dm
	Roots after 25 h incubation	
Length (mm tip^{-1})	8.8 ± 1.1^{7}	7.6 ± 1.0^{5}
	Roots excised after 25 h incubation	
Fresh weight (mg tip^{-1})	$\underline{2.8 \pm 0.4}^{9a}$	$\underline{2.0 \pm 0.4}^{12}$
Respiration rate (μmole O_2 min^{-1} g FW^{-1})	$\underline{1.20 \pm 0.18}^{5a}$	$\underline{0.86 \pm 0.16}^{5}$
Sugar content (*μmole g FW^{-1}*)		
Glucose	72 ± 14^{16a}	73 ± 24^{9}
Fructose	$\underline{30 \pm 8}^{16b}$	$\underline{20 \pm 11}^{9}$
Sucrose	34 ± 6^{16a}	39 ± 13^{9}
Starch	$\underline{11.4 \pm 2.6}^{8a}$	$\underline{3.5 \pm 0.7}^{7}$
UDP-glucose	$\underline{0.17 \pm 0.01}^{4b}$	$\underline{0.16 \pm 0.02}^{2}$
Glucose 6-P	0.59 ± 0.04^{8b}	0.58 ± 0.1^{6}
Enzymatic activities (*μmole hexose min^{-1} g FW^{-1}*)		
Sucrose synthase	$\underline{0.38 \pm 0.09}^{3b}$	$\underline{0.02 \pm 0.02}^{2}$
Neutral invertase	$\underline{0.34 \pm 0.07}^{4b}$	$\underline{0.23 \pm 0.06}^{3}$
Acid invertase	$\underline{4.39 \pm 0.37}^{3b}$	$\underline{2.76 \pm 0.56}^{3}$
Glucokinase	0.81 ± 0.23^{3b}	1.11 ± 0.19^{4}
Glucose 6-phosphatase	0.84 ± 0.14^{3a}	0.85 ± 0.28^{3}

Note: Maize root tips were incubated for 25 h with 200 mM glucose. Values represent the average ± SD and the superscript number indicates the number of replicate experiments. Underlined values are significantly different between W22wt and W22dm at the $P < 0.05$ level (Tukey's Studentized range test).

[a]Previously reported by Alonso et al. (2005).

[b]Previously reported by Alonso et al. (2007).

3.3. Defining the metabolic network

As the first step computer-aided modeling for flux quantification, the metabolic network was defined from information available in the literature and from labeling data (see Table 2). The metabolic network used in the present work (Fig. 1) is derived from, and very similar to that used for maize root tips of the Dea cv. by Dieuaide-Noubhani et al. (1995). This model includes the cytosolic and the plastidial glycolytic pathways. Plastidic glycolysis was set to be irreversible, because the amyloplasts lack fructose 1,6 bisphosphatase (Entwistle and ap Rees, 1988, 1990; Borchert et al., 1993) and the other enzyme able to convert fructose 1,6-bisP to fructose 6-P, the PPi-dependant phosphofructokinase is strictly cytosolic (Turner and Plaxton, 2003). A major difference is the addition of the new substrate cycle between hexose-P and Glc described by Alonso et al. (2005). As in Dea, the significant difference observed between sucrose and starch enrichments (Table 2) indicates that the cytosolic and plastidic hexose-P are not rapidly exchanged. The reduced labeling in the C1 position of hexose-P and in triose-P (see the labeling of alanine, Table 2A) compared to that of the [1-^{13}C]-Glc supplied as substrate, indicates the operation of the pentose phosphate pathway (PPP). This was confirmed by the transfer of label from C2 to C1 after [2-^{13}C]-Glc labeling (Table 2B). Dieuaide-Noubhani et al. (1995) suggested that the PPP was mainly located in the plastid of maize root tips. A substantial loss of label in the carbon C1 of starch glucosyl after labeling with [1-^{13}C]-Glc (Table 2A), and the limited transfer of label from C2 to C1 observed in sucrose and Glc after labeling with [2-^{13}C]-Glc (Table 2B) support this conclusion. Moreover, Debnam and Emes (1999) showed that the enzymes of the non-oxidative PPP are restricted to the plastid in maize roots. The reverse fluxes of the non-oxidative reactions of the PPP can be quantified from [2-^{13}C]-Glc labeling data and were also included. Minor pathways, like the cytosolic transaldolase reaction and the channeling of plastidic hexose-P (Dieuaide-Noubhani et al., 1995) were omitted. In animal and bacterial cells (Chance et al., 1983), but also in plants (Salon et al., 1988; Brouquisse et al., 1992), alanine, glutamate and aspartate are considered to be in equilibrium with pyruvate, α-ketoglutarate and oxalacetate, respectively. Thus the ^{13}C distribution in these amino acids reflects the distribution in the corresponding α-ketoacids. Glutamate C4 originates from acetyl-CoA whereas glutamate C2 and C3 originate from oxalacetate C3 and C2, respectively. Regarding the flow of carbon into the TCA cycle, the lower enrichment of glutamate carbons C2 and C3 compared to C4, after supplying [1-^{13}C]-Glc (Table 2A) implies that a diluting flux, attributed to the

Table 2
Steady-state ^{13}C enrichments (%) of carbohydrate and amino acid carbons after incubating root tips with [1-^{13}C]-Glc (A) or [2-^{13}C]-Glc (B)

	Glucose	Sucrose		Starch glucosyl	Alanine	Glutamate
		Glucosyl	Fructosyl			
(A) W22wt						
C1	78.6±2.7[5a]	76.6±1.1[5a]	73.8±1.8[5a]	58.3±9.6[4]	n.d.	n.d.
C2					3.8±2.2[3]	28.6±2.3[3]
C3					40.0±1.3[3]	27.6±2.0[3]
C4						36.4±1.3[3]
C5						n.d.
C6	15.5±1.7[5a]	17.8±1.6[5a]	19.9±1.3[5a]	23.8±3.4[4]		
W22dm						
C1	77.3±1.7[4]	76.5±1.9[4]	72.9±1.5[4]	70.2±9.5[4]	n.d.	n.d.
C2					6.0±2.6[3]	30.8±1.5[4]
C3					40.4±0.8[3]	28.8±0.8[4]
C4						38.8±1.7[4]
C5						n.d.
C6	15.0±1.2[4]	17.9±0.9[4]	19.9±0.8[4]	23.8±4.1[4]		
(B) W22wt						
C1	4.6±0.5[3]	5.4±0.8[3]	5.3±0.7[3]	11.3±1.2[2]	n.d.	n.d.
C2	73.3±11.9[3]	75.6±4.0[3]	74.3±2.6[3]	63.3±0.7[2]	36.9±3.7[2]	12.9±2.5[2]
C3	n.d.	n.d.	4.0±0.4[3]	n.d.	7.0±1.7[2]	13.7±3.7[2]
C4	n.d.	2.3±0.2[3]	n.d.	n.d.		6.8±1.3[2]
C5	14.9±2.1[3]	19.8±0.3[3]	20.0±0.5[3]	28.0±2.7[2]		35.0±3.5[2]
C6	2.0±0.2[3]	2.3±0.2[3]	2.4±0.4[3]	3.6±0.4[2]		
W22dm						
C1	5.4[1]	5.0[1]	4.7[1]	10.8[1]	n.d.	n.d.
C2	77.7[1]	73.6[1]	70.8[1]	73.7[1]	34.3[1]	11.6[1]
C3	n.d.	n.d.	n.d.	n.d.	7.6[1]	14.8[1]
C4	n.d.	n.d.	n.d.	n.d.		8.0[1]
C5	16.9[1]	19.9[1]	20.5[1]	26.9[1]		n.d.
C6	2.0[1]	2.2[1]	2.3[1]	4.3[1]		

Notes: In (A), the enrichments of carbons C2–C5 of the carbohydrates are within 0.6% of the natural abundance level of 1.1% and are not reported. Values are the average±SD and the superscript number specifies the number of experiments. n.d. means not determined.
[a]Previously reported by Alonso et al. (2005).

phosphoenolpyruvate (PEPC), enters the tricarboxylic acid cycle (Dieuaide-Noubhani et al., 2007).

3.4. Flux quantification

The rate of Glc consumption was determined after incubation of the root tips with [U-^{14}C]-Glc for 5, 10, 15 and 20 min (Fig. 2A). In W22wt, the rate of Glc consumption was 360 ± 48 nmole hexose min^{-1} g FW^{-1}, which is not significantly different from that measured in W22wt root tips (394 ± 73 nmole hexose min^{-1} g FW^{-1}).

To quantify the unidirectional rates of sucrose and starch synthesis, W22dm root tips were incubated with [U-^{14}C]-Glc for 15, 30 and 60 min. The amount of starch and sucrose produced after 15, 30 and 60 min (Fig. 2C and D) were calculated using Eq. (1) described by Alonso et al. (2005) from the amount of radioactivity incorporated into sucrose and starch glucosyl units, respectively, and from the SR of their precursor, Glc-6-P (Fig. 2B). As underlined by Alonso et al. (2005), the immediate precursors of sucrose and starch are UDP-Glc and ADP-Glc. Glc-6-P is classically used as the indicator of UDP-Glc specific radioactivity, because they are in rapid exchange, through the UDP-Glc pyrophosphorylase and hexose-P isomerase reactions (Geigenberger et al., 1997; Roscher et al., 1998). This approximation was validated by the comparison of the increase of the SR measured in Glc-6-P and UDP-Glc (Fig. 2B) in W22dm: as previously observed for the W22wt (Alonso et al., 2005), no significant differences were found between the SR of Glc-6-P and UDP-Glc. In W22dm, the unidirectional rate of sucrose synthesis, V_{suc}, was estimated at 224 ± 49 nmole min^{-1} g FW^{-1}. The SR of ADP-Glc was not measured; assuming it was the same as that of Glc-6-P, the unidirectional rate of starch synthesis was found to be between 19 and 23 nmole min^{-1} g FW^{-1}, which is not significantly different from that obtained with W22wt root tips (Table 3). Due to the slow exchange of the cytosolic and plastidial pool of hexose-P, ADP-Glc labeling may be lower than that of Glc-6-P. We therefore cannot exclude that the flux toward starch synthesis was underestimated.

The rate of cell wall polysaccharide synthesis was measured by incubating W22dm root tips for 15, 30 and 60 min with [U-^{14}C]-Glc. The unidirectional rate of synthesis of cell wall polysaccharides (Fig. 2E) was

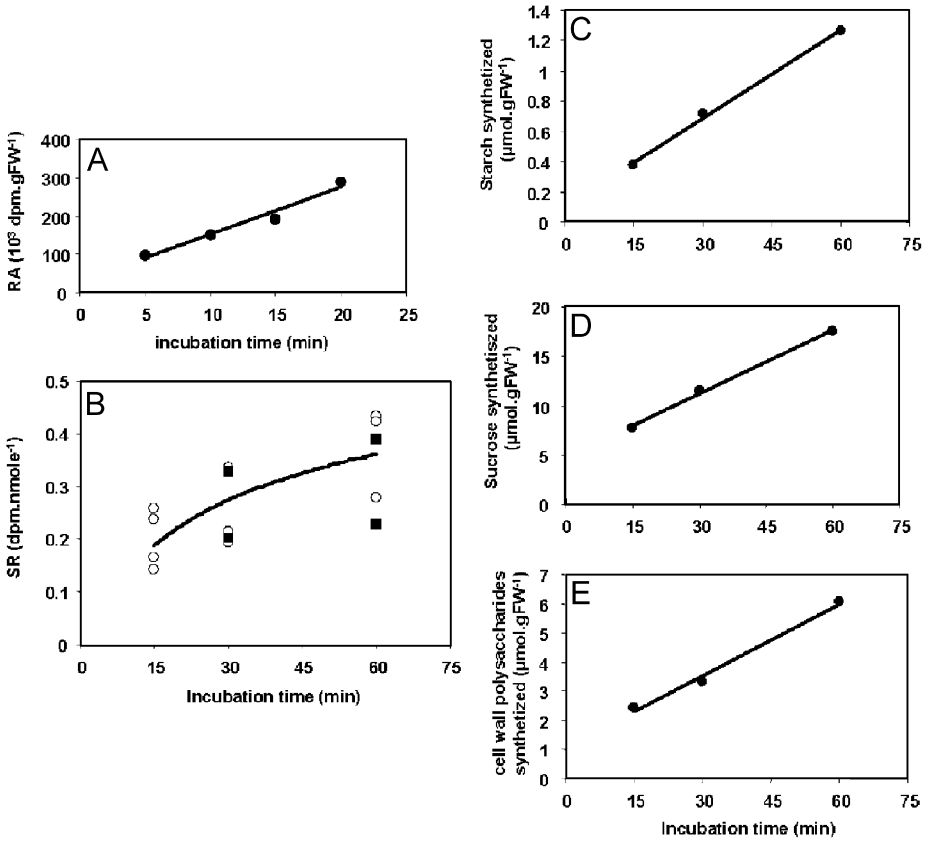

Fig. 2. Short time labeling experiments for the quantification of the glucose uptake, and of the rates of cell wall, starch and sucrose syntheses by W22dm maize root tips. In all experiments, maize root tips were incubated with 200 mM Glc for 25 h before being transferred into a medium containing 200 mM [U-^{14}C]-Glc. (A) Glc uptake: Root tips were incubated with [U-^{14}C]-Glc (30 dpm nmole^{-1}) for 5, 10, 15 and 20 min. Maize root tips were then ground and radioactivity was measured by scintillation counting. These data are from one representative experiment of two similar replicates. (B) specific radioactivity of Glc-6-P (○) and UDP-Glc (■). Root tips were incubated with [U-^{14}C]-Glc (100–200 dpm nmol^{-1}) for 15, 30 and 60 min. The specific activity of Glc-6-P and UDP-Glc were obtained as described in the Methods section. The symbols correspond to two sets of values obtained in two independent experiments. (C–E) starch (C), sucrose (D) and cell wall (E) synthesis: W22dm root tips were incubated with [U-^{14}C]-Glc (30 dpm nmol^{-1}) for 15, 30, 60 min. The quantities of radioactivity incorporated into glucosyl moieties of sucrose and starch and into polysaccharides during a time interval were then converted to the amount of sugar produced, expressed in mol g FW^{-1} as described in Material and methods. The results shown are from a typical representative experiments, which were repeated 5, 1 and 2 times for sucrose, starch and cell wall polysaccharides, respectively. These data were used to quantify the unidirectional rate of sucrose, starch and cell wall polysaccharide syntheses.

found to be 76 ± 5 nmole min^{-1} g FW^{-1} in W22dm root tips, which is significantly higher than in W22wt (52 ± 14 nmole min^{-1} g FW^{-1}; Table 2).

The other fluxes described in Fig. 1 were calculated from metabolite enrichments after steady-state labeling experiments with [1-^{13}C]-Glc or [2-^{13}C]-Glc (Table 2) using the software 13C-FLUX (Wiechert and de Graaf, 1997; Wiechert et al., 1997, 1999; Möllney et al., 1999) as described in Material and methods. The software 13C-FLUX evaluates a set of stoichiometrically feasible fluxes that best accounts for the metabolite enrichments and the pulse labeling data. To ensure that the evaluated set of fluxes is an optimum rather than a local minimum, the flux optimization was repeated over 400 times from different starting points. For W22wt and W22dm, respectively, 78% and 64% of the optimization runs converged to a very similar set of best fit flux values. Confidence intervals for each flux were determined from the range of measured labeling values obtained in different experiments and the sensitivity of each flux value to variation in the different measurements. The value and the confidence interval for each flux are listed in Table 3. Interestingly, the flux values V_{wall}, V_{suc}, V_{sta}, determined as described above and V_{res} ($V_{res} = V_{suc} + V_{gpase}$), determined in a first approach as in Alonso et al. (2005), which were parameters for the calculation of fluxes but set as free in the 13C-FLUX model were not significantly modified after their recalculation (data not shown). Most of the fluxes are strikingly similar in W22wt and W22dm. In both lines, 20% of the Glc taken up goes through the oxidative steps of the PPP and the fluxes through the substrate cycles (V_{suc}, V_{gpase}, V_{ald}, V_{sts}) are not significantly different between the lines. For both W22wt and W22dm, the main substrate cycle is the resynthesis of Glc from Glc-6-P (V_{gpase}) and this flux is 6–8 times higher than the rate of Glc uptake.

In contrast, four fluxes appeared to be reduced as a consequence of the reduction of SuSy activity: V_{gf} (flux catalyzed by Glc-6-P isomerase), V_{gly} (glycolytic flux

Table 3
Metabolic fluxes in W22wt and W22dm maize root tips

		W22wt		W22dm	
		Forward	Backward	Forward	Backward
Pulse labeling experiments (nmole hexose min^{-1} g FW^{-1})					
V_g	Rate of glucose uptake	394±73[a]	0	360±48[3]	0
V_{suc}	Fluxes of sucrose synthesis and degradation	178±36[a]	⩽178±36[a]	224±49[6]	⩽224±49
V_{sts}	Fluxes of starch synthesis and degradation	30±11[a]	⩽30±11[a]	21±2[2]	⩽21±2
V_{wall}	Rate of wall synthesis	52±14[a]	0	76±9[3]	0
Steady-state labeling experiments (nmole min^{-1} g FW^{-1})					
V_{res}	Fluxes from G6P to glucose ($V_{suc}+V_{gpase}$)	2241±481	0	2464±614	0
V_{hk}	Flux through hexokinase	2635±481	0	2824±614	0
V_{gf}	Fluxes catalyzed by G6P isomerase	8789±364	8601±320	2395±185	2265±144
V_{ald}	Fluxes catalyzed by aldolase	409±55	222±11	331±50	202±11
V_{gly}	Glycolytic flux	647±28	0	539±10	0
V_{hcp}	Exchange of cytosolic and plastidic hexose-P	412±75	263±32	381±68	230±29
V_{ppp1}	Flux of the oxidative pentose-P pathway	81±7	0	71±9	0
V_{ppp2}	Fluxes catalyzed by transketolase	39±10	12±8	35±16	11±13
V_{ppp3}	Fluxes catalyzed by transaldolase	180±38	153±35	152±40	128±37
V_{ppp4}	Fluxes catalyzed by transketolase	27±11	0±9	24±16	0±13
V_{aldp}	Fluxes catalyzed by plastidic aldolase	122±42	0	128±39	0
V_{pk}	Oxidative flux through PK	349±33	0	332±14	0
V_{pepc}	Anaplerotic flux through PEPC	298±34	0	207±15	0
V_{pdh}	Flux catalyzed by pyruvate DH	478±56	0	441±24	0
V_{cs}	Flux through citrate synthase	478±56	0	441±24	0
V_{ca}	Flux catalyzed by aconitase	478±56	0	441±24	0
V_{glu}	Rate of glutamate synthesis	84±27	0	49±12	0
V_{sfa}	Flux through 2-oxoglutarate DH	394±80	0	392 ±35	0
V_{fum}	Flux catalyzed by fumarase	6621±1121	6227±1067	2957±337	2565±301
V_{asp}	Rate of aspartate production	84±27	0	49±12	0
V_{me}	Flux through malic enzyme	129±33	0	109±21	0
V_{Co_2}	Rate of CO_2 production	1262±242	0	1249±105	0

Notes: Fluxes are given in nmole molecule min^{-1} g FW^{-1}. The values are the best fit and also the most frequently determined optimized flux values±confidence range. ND: not determined.
[a]Results previously reported by Alonso et al. (2005).

measured at the triose-P to PEP segment of glycolysis), V_{pepc} (anaplerotic flux) and V_{fum} (flux catalyzed by fumarase) which were found to be 73%, 17%, 31% and 55% lower, respectively, in the double mutant than in the wild type. However, the decrease in V_{gf} and V_{inv} were not significant because in the range of observed values, large variations of the fluxes V_{fg} and V_{fum} may result from minor changes in the experimental enrichments of the sucrose glucosyl and fructosyl carbons used in the calculation. The increase in the PK/PEPC flux ratio indicates that more of the phosphoenolpyruvate produced by glycolysis is directed to respiration in the double mutant. The decrease of the PEPC reaction suggests a decrease of the biosynthetic activities, mainly the biosynthesis of amino acids.

3.4.1. Model validation

A way to estimate the validity of our metabolic network is to run a χ^2-test in order to check if the model effectively describes the observed measurements. According to Dauner et al. (2001) the probability distribution for different values of χ^2 can be derived analytically and is the χ^2 distribution for $n_{freedom} = n_{total} - m_{total}$ (Eq. (18); Dauner et al., 2001), where $n_{freedom}$ is the degrees of freedom, n_{total} the number of measurements and m_{total} the number of estimated parameters. In our case, $n_{freedom} = 57-14$ for W22wt and $n_{freedom} = 55-14$ for W22dm. With a confidence level of 95%, the χ^2 criterion is ⩽59.3 and 56.9 for W22wt and W22dm, respectively. The calculated χ^2 values of 39.8 and 55.2 for W22wt and W22dm, respectively, are beneath the χ^2 criterion. Thus with a confidence of 95% the χ^2 test is satisfied for both W22wt and W2dm, which indicates that our metabolic network describes the labeling data well.

Because substrate cycles are ATP wasting, we verified that the balance of ATP production and its consumption by the substrate cycles was positive. ATP production can be estimated from the respiration rate assuming that the complete oxidation of 1 mole of Glc leads to the formation of 30 mole of ATP (Geigenberger and Stitt, 1991). According to the respiration rates (Table 1) ATP production is about 6000±900 and 4300±800 nmole min^{-1} g FW^{-1} for W22wt and W22dm root tips, respectively. ATP consumption can be estimated for each substrate cycle: (i) cycling of each Glc via Glc-6-phosphatase (V_{gpase}) costs 1 ATP; (ii) the sucrose cycle (V_{suc}) requires 1–3 molecules of ATP per

molecule of sucrose, depending on the enzymes involved (here we have considered sucrose degradation by invertase and sucrose synthesis by saccharose phosphate synthase, which leads to the consumption of 2 molecules of ATP per molecule of sucrose if PPi is consider as phosphate donor (Hill and ap Rees, 1994; Dieuaide-Noubhani et al., 1995; Trethewey et al., 1999); (iii) starch synthesis and degradation (V_{sts}) requires 1 ATP for each transformation of Glc-1-P into ADP-Glc via ADP-Glc pyrophosphorylase; (iv) in triose-P/hexose-P cycling (V_{ald}), 3 enzymes can be involved: ATP-dependent phophofructokinase, fructose 1,6-bisphosphatase and PPi-dependent phosphofructokinase. ATP consumption by this substrate cycle is difficult to estimate since we do not know the contribution of each one of the enzymes cited above. In consequence, we can consider the maximal consumption of ATP by the triose-P/hexose-P cycle with ATP-dependent phosphofructokinase and fructose 1,6-bisphosphatase. This assumption only has a low impact on total ATP consumption because the triose-P/hexose-P cycle is a relatively minor flux. According to Table 3, Glc-6-P, sucrose, starch and triose-P/hexose-P cycles consumed, respectively, 2063 ± 445, 356 ± 72, 30 ± 11, and 222 ± 11 nmole min^{-1} g FW^{-1} for W22wt and 2240 ± 565, 448 ± 98, 21 ± 2 and 202 ± 11 nmole min^{-1} g FW^{-1} for W22dm. The fluxes of substrate cycling measured in the root tips, consume 44% and 67% of the ATP produced in W22wt and W22dm maize root tips, respectively.

The increase in the flux V_{wall} measured from C14 labeling suggests an increase of the content of cell wall polysaccharides in the double mutant. This result is surprising because a decrease in cellulose, and other cell wall polysaccharides was expected in response to the absence or decreased activity of two of three sucrose synthase isozymes in the double mutant (Chourey et al., 1998; Haigler et al., 2001). In order to observe possible differences in the composition of the cell walls, polysaccharides from [U-^{13}C]-Glc labeled maize root tips were analyzed on residues obtained after ethanolic and starch extractions by CP-MAS ^{13}C-NMR spectroscopy (Fig. 3A and B). The spectra are characteristic of cell walls with resonances between 10 and 50 ppm assigned to aliphatic carbons from phospholipids and proteins. Resonances between 50 and 120 ppm are almost entirely from cell wall compounds (cellulose, hemicellulose and pectins) while those between 120 and 170 ppm are due to polyphenols and at 170–190 ppm to carbonyl and carboxyl groups in polysaccharides and proteins. Qualitatively, there is no difference between these two spectra (Fig. 3), indicating that cell wall components were the same in the wild type and the double mutant. Quantitative analysis of these

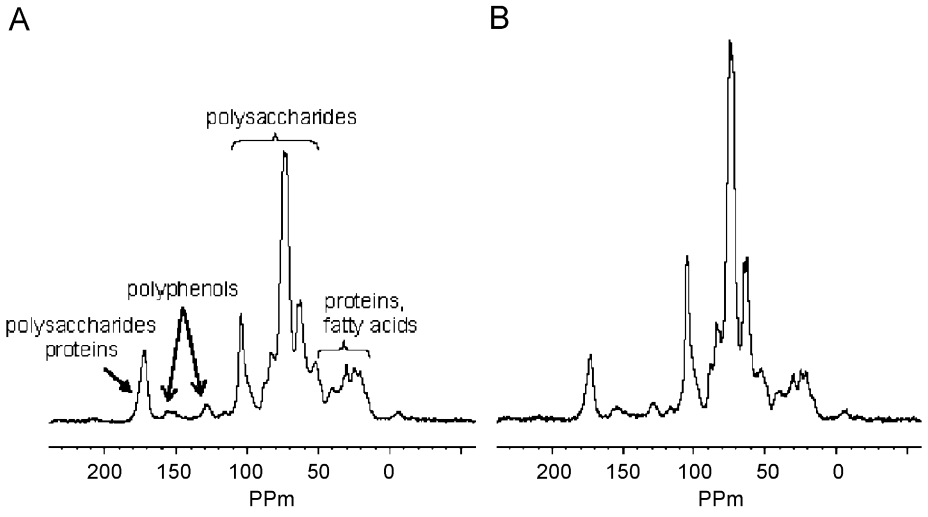

C

	W22wt	W22dm
Rhamnose	0.1 - 0.1	nd - 0.1
Fucose	0.2 - 0.2	0.3 - 0.2
Arabinose	3.6 - 3.9	4.2 - 3.9
Xylose	6.7 - 7.5	8.8 - 8.6
Mannose	0.5 - 0.6	0.5 - 0.6
Galactose	3.1 - 3.2	3.0 - 2.9
Glucose	18.9 - 20.5	22.0 - 25.4
AAG	1.3 - 1.4	1.5 - 1.4
Total sugars	34.6 - 37.4	40.2 - 43.2

Fig. 3. Analysis of cell wall polysaccharides. Maize root tips incubated 25 h with [U-^{13}C] glucose. Ethanol-soluble compounds and starch were removed as described in Material and methods. C-PMAS spectra were performed on lyophilized residues obtained from W22wt (A) and W22dm (B). The sugar composition of polysaccharides determined after acidic hydrolysis of the sample is given in (C). The quantity of sugar was expressed in mg of sugar/100 mg FW. Data are from two independent experiments.

spectra, after normalization by dividing by the fresh weight of maize root tip, clearly shows an increase of the peak area of the peaks of cell wall polysaccharides in the double mutant. The quantification of individual sugars after acidic hydrolysis (Fig. 3C) indicates an increase of 16% in cell wall polysaccharides (cellulose, hemicelluloses, pectins) in the double mutant compared to W22wt. The similarity of the increase in cell wall polysaccharides content and in the V_{wall} flux determined from ^{14}C labeling experiments indicates that the increase in the unidirectional flux of synthesis measured in the double mutant is not accompanied by an increased cell wall degradation.

The increase in cell wall polysaccharide content in the double mutant implies an increase in the cell wall/cell volume ratio, which may be a consequence of the reduced cell size in the double mutant. The number of cell per root could not be determined precisely because maize root tips are heterogeneous. However, the analysis of cell size in a similar region of the root showed a reduction of cell size in the double mutant (Fig. 4) which is in agreement with the hypothesis that the smaller size of the roots in the double mutant is related with a decreased cell size. Therefore, the increase of the rate of cell wall synthesis (Table 3) in W22dm is corroborated by experimental data showing higher levels of cell wall polysaccharides (Figs. 3 and 4).

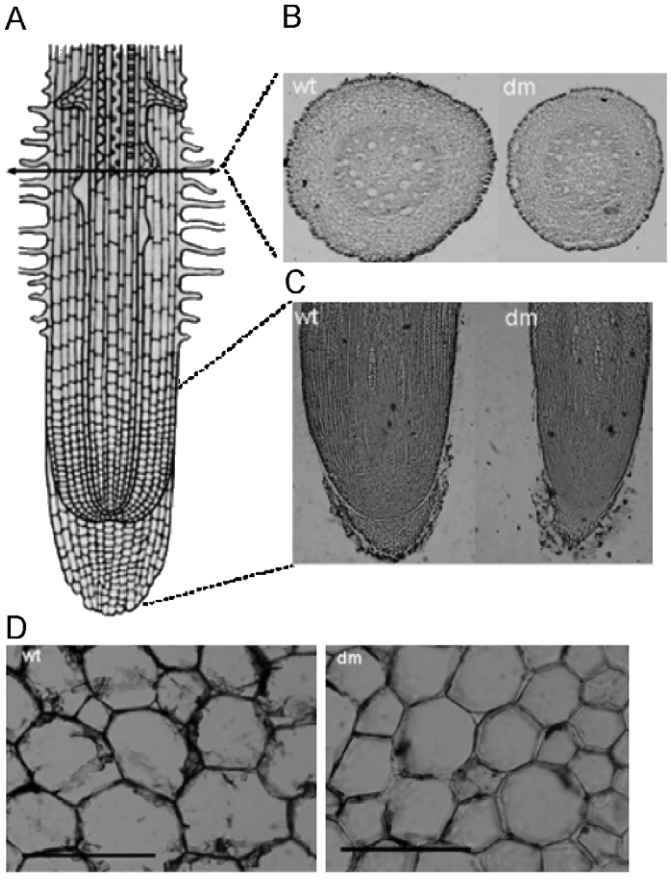

Fig. 4. Histological analysis of maize root tips: (A) schematic view of maize root tips showing the level of longitudinal and cross sections. (B) Transversal sections through W22wt (left) and W22dm (right) root tips. (C) Longitudinal section through W22wt (left) and W22dm (right) root tips. (D) Magnifications of (B). Bars = 100 μm. Maize root tips were stained with toluidine blue.

4. Discussion

In maize root tips, sucrose enters the cells by the apoplastic pathway, essentially as free Glc and fructose, after hydrolysis by the cell wall invertase (Bret-Harte and Silk, 1994). Thus, the function of SuSy is the interconversion of the sucrose, UDP-Glc and fructose pools present in the cytosol rather than the degradation of entering sucrose. The clear phenotype of the root tips of the sucrose synthase *sh1 sus1* double mutant, which retains 5% of the weight of total sucrose synthase activity but present a reduced diameter and a decreased starch content (see results, Table 1), indicates that SuSy does play a role in the regulation of their metabolism. In order to establish whether the mutation of the sucrose synthase genes affects cell wall polysaccharides, starch biosynthesis or central metabolism, metabolic fluxes were measured through a combination of two experimental methods: (i) unidirectional rates of cell wall polysaccharides, starch and sucrose syntheses were measured through short time labeling experiments with [U-^{14}C]-Glc; and (ii) fluxes at different steps of central metabolism were determined after isotopic steady-state labeling ([U-^{13}C]-, [1-^{13}C]-, or [2-^{13}C]-Glc), and carbon enrichment assays through ^{1}H and ^{13}C NMR.

This approach is similar to that used by Alonso et al. (2005) to study the sugar-hexose-P interconversion. In the present work, an additional labeling with [2-^{13}C]-Glc was used to quantify the more complex network which involves glycolysis, the pentose-P pathway, and the TCA. As validated by the χ^2-test, thanks to the combination of different labeling experiments it was possible to build a model that accounts for the measurements obtained in both W22wt and W22dm maize root tips.

4.1. Sh1 and Sus1 mutations slightly affect the central metabolism

The results show that the reduction of the respiratory rate observed in W22dm is associated with a reduction of the glycolytic flux and of the PEPC activity by about 30% which is reflected by a decrease in V_{asp} and V_{glu}, the calculated fluxes of biosynthesis of amino acids of the aspartate and glutamate families. This indicates a decrease in the metabolic activity of the double mutant. On the other hand, the fluxes in the substrate cycles were not significantly affected. Due to the reduction of the respiratory rate, maintaining the activity of substrate cycles would reduce the ATP availability for biosynthetic process. In addition, no effect on the pentose phosphate pathway, and therefore on the NADPH supply, was apparent since no significant reduction in V_{ppp1} was observed in W22dm compared to wt (Table 3).

4.2. SH1 and SUS1 are not specific providers of UDP-Glc for cell wall synthesis in maize root tips

In heterotrophic plant tissues a major fate of the UDP-Glc produced by the SuSy reaction is used for cellulose synthesis. In cotton fibres, UDP-Glc is channeled to cellulose synthesis by a SuSy protein bound to cellulose synthase (Haigler et al., 2001). This model is usually considered to be valid in other plant systems as well. In maize endosperm, Chourey et al. (1998) attributed the *sh1* phenotype to defect in cellulose synthesis, and SH1 was found to be bound to membranes in relation with cellulose synthesis (Duncan et al., 2006 and refs therein). A decrease in the rate of cellulose synthesis is therefore expected in W22dm which lacks SH1 and SUS1. Surprisingly, we observed that, although the diameter and growth rate of W22dm root tips are lower than in the wild type (Table 1), the amount of cell wall polysaccharides (cellulose, hemicellulose and pectins) content per milligram FW was increased. According to pulse labeling experiments, this increase was correlated with an increase in the unidirectional rate of cell wall synthesis. Because SuSy is involved in the synthesis of cellulose and, in young maize plants, cellulose only accounts for 47% of cell wall polysaccharides (McDermitt and Loomis, 1981), the increased flux V_{wall} might be explained by an increase in non-cellulose polysaccharides over-compensating the absence of cellulose synthesis. This was not verified by the analysis of cell walls by CP-MAS ^{13}C-NMR spectroscopy and sugar analysis, since no qualitative difference was observed in the composition of cell wall between W22wt and W22dm (Fig. 3). Thus, the increase of V_{wall} in the double mutant reflects an increase of the rate of cellulose synthesis. Two hypotheses can be proposed to explain this surprising result. The residual SuSy activity was found to be much higher in the root tips (about 5% of wild type, Table 1) than in the endosperm (only 0.5% of wild type, Chourey et al., 1998). It is probably due to the third gene, *Sus2*, which is expressed in roots (Carlson et al., 2002; Subbaiah et al., 2006). In the wt, SUS2 exists as hetero-oligomers with SUS1. These oligomers are not membrane-bound and SUS2 was considered to prevent SUS1 from providing UDP-Glc for cellulose synthesis (Duncan et al., 2006). Conversely, SUS2 alone was found to bind to membranes *in vitro* but whether it binds to cellulose synthase is not known. However, since the SuSy activity measured in W22dm root tips (Table 1) was lower than the estimated rate of cellulose synthesis (Table 3), this contribution to cellulose synthesis would be minor. Alternatively, UDP-Glc needed for cellulose synthesis could be provided by the near equilibrium UDP-Glc pyrophosphorylase reaction.

4.3. SuSy does not provide ADP-Glc for starch synthesis in maize root tips

The low starch content in W22dm root tips is in agreement with similar observations of decreased in starch content in W22dm developing endosperm (Chourey et al., 1998), and in SuSy antisensed potato tuber (Zrenner et al., 1995), and tomato fruit (Chengappa et al., 1999). In tomato fruit, the correlation between starch content and SuSy activity is positive but very weak ($R = 0.54$) (Wang et al., 1993). In most studies only strong reductions of SuSy activity (70% in potato tuber and more than 99% in tomato) led to decreased starch contents (Zrenner et al., 1995; Chengappa et al. 1999). These results raise the question of the link between the decreases in SuSy activity and in starch content.

Classically, ADP-Glc is produced in the plastid in an ADP-Glc pyrophosphorylase (AGPase) reaction which uses Glc-1-P imported (sometimes as Glc-6-P) from the cytosol via a hexose-P translocator. Recently, however, two AGPase have been identified in cereal endosperm, one plastidial, the other cytosolic. In maize endosperm, 95% of the AGPase is cytosolic and a translocator for ADP-Glc is required to allow starch synthesis (Baroja-Fernandez et al., 2003, 2004). Recently, Baroja-Fernandez et al. (2003) hypothesized that SuSy might be the major enzyme involved in ADP-Glc synthesis in barley endosperms and potato tubers. In potato with reduced SuSy expression, Zrenner et al. (1995) observed no change in AGPase enzyme activity, in spite of a reduction in the amount of AGPase mRNA, and therefore did not attribute the reduction in starch content to a decrease in the rate of starch biosynthesis. Baroja-Fernandez et al. (2003) suggested that the decrease of starch could be due to the decrease of SuSy activity. This hypothesis was supported by a decrease in ADP-Glc content whereas the Glc-6-P pool was unchanged. A similar hypothesis could be proposed for maize root tips, but is not supported by our results. First, the unidirectional rate of starch synthesis, measured from pulse labeling experiments, is not reduced in the double mutant in spite of the decrease in SuSy activity (Table 3). It is thus probable that the decrease of starch is due to an increase of its turnover and not to a substrate limitation related to the decrease of SuSy. Secondly, the different labeling of starch- and sucrose-glucosyl units observed after steady-state labeling (Table 2A and B) clearly indicates that starch and sucrose are made from different Glc-P pools; if ADP-Glc was made in the cytosol by either SuSy or a cytosolic AGPase, sucrose and starch would be identically labeled. Attempts to include even a small flux of cytosolic ADP-Glc production in our model failed, thus showing that no significant flux of ADP-Glc from the cytosol is consistent with our labeling data. Since maize root only accumulate small amounts of starch, and the cytosolic production of ADP-Glc was hypothesized for starch storing organs like maize (Denyer et al., 1996), barley or rice endosperm, or potato tubers (Baroja-Fernandez et al., 2003; Johnson et al., 2003; Patron et al., 2004), our data may not apply to specialized starch storing organs. This conclusion agrees with the recent publication (Toyota et al., 2006) showing that, in rice, of the three genes coding for a putative ADP-

Glc translocator, one is expressed in seed only, and the other two mainly in leaves but the genes coding for hexose-P translocators are similarly expressed in leaves, seeds and roots.

5. Conclusion

The detailed study of the central metabolism of the W22dm sucrose synthase double mutant, where only the *Sus2* gene produces an active SuSy protein, was undertaken as a means to evaluate potential specific roles of the inactivated genes, *Sus1* and *Sh1*. Steady-state labeling experiments showed limited effects of the double mutation on the central metabolism, including at the level of the sucrose-hexose-P exchanges. They led to the detection of a decrease in the rate of the PEPC reaction which suggests a decreased net rate of amino acid synthesis, which is in agreement with the decreased rates of respiration and growth but has no obvious relation with the sucrose synthase reaction. Steady-state label distribution of starch glucosyl was found to be different from that of sucrose units, which suggests that the ADP-Glc for starch synthesis is build up inside the plastid, rather than in the cytosol. In contrast, the direct effects of the double sucrose synthase mutations on starch or cellulose synthesis, which were expected from previous studies, were not confirmed. Instead, pulse labeling showed that the suppression of SUS1 and Sh1 did not result in any decrease in the rates of starch or cellulose synthesis. It remains possible that SUS1 and Sh1 proteins do have specialized functions in the wild type cells, but our results suggest that either the SUS2 isozyme, which is not associated with membranes *in vivo* (Duncan et al., 2006), is able to replace the other two isoforms in the double mutant, or UDP-Glc is produced by alternative pathways. This is a striking illustration of the flexibility of plant metabolism.

Acknowledgments

Access to the NMR facilities of the BIBS platform (Biopolymères Interactions Biologie Structurale) of INRA-Nantes and to the Metabolome-Fluxome facility of IFR 103 BVI-Bordeaux was greatly appreciated by the authors. Special thanks are due to Mickaël Maucourt (Metabolome-Fluxome facility) for technical advice and his help with the setup of NMR analyses with the cryoprobe system.

References

Alonso, A.P., Vigeolas, H., Raymond, P., Rolin, D., Dieuaide-Noubhani, M., 2005. A new substrate cycle in plants. Evidence for a high glucose-phosphate-to-glucose turnover from in vivo steady-state and pulse-labeling experiments with [^{13}C]glucose and [^{14}C]glucose. Plant Physiol. 138 (4), 2220–2232.

Alonso, A.P., Raymond, P., Rolin, D., Dieuaide-Noubhani, M., 2007. Substrate cycles in the central metabolism of maize root tips under hypoxia. Phytochemistry 68, 2222–2231.

Baroja-Fernandez, E., José Muñoz, F., Saikusa, T., Rodriguez-Lopez, M., Akazawa, T., Pozueto-Romero, J., 2003. Sucrose synthase catalyzes the de novo production of ADPGlucose linked to starch biosynthesis in heterotrophic tissues of plants. Plant Cell Physiol. 44, 500–509.

Baroja-Fernandez, E., José Muñoz, F., Zandueta-Criado, A., Moran-Zorzano, M.T., Viale, A.M., Alonso-Casajus, N., Pozueto-Romero, J., 2004. Most of ADP-glucose linked to starch biosynthesis occurs outside the chloroplast in source leaves. PNAS 101, 13080–13085.

Bereterbide, A., Hernould, M., Farbos, I., Glimelius, K., Mouras, A., 2002. Restoration of stamen development and production of functional pollen in an alloplasmic CMS tobacco line by ectopic expression of the *Arabidopsis thaliana* SUPERMAN gene. Plant 29, 607–615.

Blakeney, A.B., Harris, P.J., Henry, R.J., Stone, B.A., 1983. A simple and rapid preparation of alditol acetates for monosaccharide analysis. Carbohyd. Res. 113, 292–299.

Borchert, S., Harborth, J., Schunemann, D., Hoferichter, P., Heldt, H.W., 1993. Studies of the enzymic capacities and transport properties of pea root plastids. Plant Physiol. 101, 303–312.

Bouny, M., Saglio, P., 1996. Glycolytic flux and hexokinase activities in anoxic maize root tips acclimated by hypoxic pretreatment. Plant Physiol. 111, 187–194.

Bret-Harte, M.S., Silk, W.K., 1994. Nonvascular, symplasmic diffusion of sucrose cannot satisfy the carbon demands of growth in the primary root tip of *Zea mays* L. Plant Physiol. 105, 19–33.

Brouquisse, R.M., James, F., Raymond, P., Pradet, A., 1991. Study of glucose starvation in excised maize root tips. Plant Physiol. 96, 619–626.

Brouquisse, R., James, F., Raymond, P., Pradet, A., 1992. Asparagine metabolism and nitrogen distribution during protein degradation in sugar-starved maize root tips. Planta 188, 384–395.

Brouquisse, R.M., Evrard, A., Rolin, D., Raymond, P., Roby, C., 2001. Regulation of protein degradation and protease expression by mannose in maize root tips. Pi sequestration by mannose may hinder the study of its signaling properties. Plant Physiol. 125, 1485–1498.

Carlson, S.J., Chourey, P.S., Helentjaris, T., Datta, R., 2002. Gene expression studies on developing kernels of maize sucrose synthase (SuSy) mutants show evidence for a third SuSy gene. Plant Mol. Biol. 49, 15–29.

Chance, E.M., Seeholzer, S.H., Kobayashi, K., Williamson, J.R., 1983. Mathematical analysis of isotope labeling in the citric acid cycle with applications to ^{13}C NMR studies in perfused rat hearts. J. Biol. Chem. 258, 13785–13794.

Chengappa, S., Guilleroux, M., Phillips, W., Shields, R., 1999. Transgenic tomato plants with decreased sucrose synthase are unaltered in starch and sugar accumulation in the fruit. Plant Mol. Biol. 40, 213–221.

Chourey, P.S., 1981. Genetic control of sucrose synthase in maize endosperm. Mol. Gen. Genet. 184, 372–376.

Chourey, P.S., 2006. Nomenclature of sucrose synthase genes and the gene products. Maize Genet. Coop. Newslett. 80, 35.

Chourey, P.S., Latham, M.D., Still, P.E., 1986. Expression of two sucrose synthetase genes in endosperm and seedling cells of maize: evidence of tissue specific polymerization of protomers. Mol. Gen. Genet. 203, 251–255.

Chourey, P.S., Taliercio, E.W., Carlson, S.J., Ruan, Y.L., 1998. Genetic evidence that the two isozymes of sucrose synthase present in developing maize endosperm are critical, one for cell wall integrity and the other for starch biosynthesis. Mol. Gen. Genet. 259, 88–96.

Dauner, M., Bailey, J.E., Sauer, U., 2001. Metabolic flux analysis with a comprehensive isotopomer model in *Bacillus subtilis*. Biotechnol. Bioeng. 76 (2), 144–156.

Debnam, P.M., Emes, M., 1999. Subcellular distribution of enzymes of the oxidative pentose phosphate pathway in root and leaf tissues. J. Exp. Bot. 50, 1653–1661.

Denyer, K., Dunlap, F., Thorbjornsen, T., Keeling, P., Smith, A.M., 1996. The major form of ADP-glucose pyrophosphorylase in maize endosperm is extra-plastidial. Plant Physiol. 112, 779–785.

Dieuaide-Noubhani, M., Raffard, G., Canioni, P., Pradet, A., Raymond, P., 1995. Quantification of compartmented metabolic fluxes in maize root tips using isotope distribution from ^{13}C- or ^{14}C-labeled glucose. J. Biol. Chem. 270, 13147–13159.

Dieuaide-Noubhani, M., Alonso, A., Rolin, D., Eisenreich, W., Raymond, P., 2007. Metabolic flux analysis. Recent advances in carbon metabolism in plants. In: Baginsky, S., Fernie, A.R. (Eds.), Plant Systems Biology. Birkhäuser Verlag, Basel, Switzerland, pp. 213–243.

Duncan, K.A., Hardin, S.C., Huber, S.C., 2006. The three maize sucrose synthase isoforms differ in distribution, localization, and phosphorylation. Plant Cell Physiol. 47, 959–971.

Englyst, H.N., Cummings, J.H., 1988. Improved method of measurement of dietary fiber as non-starch polysaccharides in plant foods. J. Assoc. Off. Anal. Chem. 71, 808–814.

Entwistle, G., ap Rees, T.A., 1988. Enzymic capacities of amyloplasts from wheat (*Triticum aestivum*) endosperm. Biochem. J. 255, 391–396.

Entwistle, G., ap Rees, T.A., 1990. Lack of fructose-1,6-bisphosphatase in a range of higher plants that store starch. Biochem. J. 271, 467–472.

Geigenberger, P., Stitt, M., 1991. Regulation of carbon partitioning between sucrose and nitrogen assimilation in cotyledons of germinating *Ricinus communis* L. seedlings. Planta 185, 563–568.

Geigenberger, P., Stitt, M., 1993. Sucrose synthase catalyses a readily reversible reaction in vivo in developing potato tubers and other plant tissues. Planta 189, 329–339.

Geigenberger, P., Reimholz, R., Geiger, M., Merlo, L., Canale, L., Stitt, M., 1997. Regulation of sucrose to starch metabolism in potato tubers in response to short-term water deficit. Planta 201, 502–518.

Gibeaut, D.N., Carpita, N.C., 1991. Tracing cell wall biogenesis in intact cells and plants. Plant Physiol. 97, 551–561.

Haigler, C.H., Ivanova-Datcheva, M., Hogan, P.S., Salnikov, V.V., Hwang, S., Martin, K., Delmer, D.P., 2001. Carbon partitioning to cellulose synthesis. Plant Mol. Biol. 47, 29–51.

Hill, S.A., ap Rees, T., 1994. Fluxes of carbohydrate metabolism in ripening bananas. Planta 192, 52–60.

James, F., Brouquisse, R., Pradet, A., Raymond, P., 1993. Changes in proteolytic activities in glucose-starved maize root tips: regulation by sugars. Plant Physiol. Biochem. 31, 845–856.

Johnson, P., Patron, N., Bottrill, A., Dinges, J., Fahy, B., Parker, M., Waite, D., Denyer, K., 2003. A low-starch barley mutant, riso 16, lacking the cytosolic small subunit of ADP-glucose pyrophosphorylase, reveals the importance of the cytosolic isoform and the identity of the plastidial small subunit. Plant Physiol. 131, 684–696.

Lowell, C.A., Tomlinson, P.T., Koch, K.E., 1989. Sucrose-metabolizing enzymes in transport tissues and adjacent sink structures in developing citrus fruit. Plant Physiol. 90, 1394–1402.

McDermitt, D.K., Loomis, R.S., 1981. Elemental composition of biomass and its relation to energy content, growth efficiency, and growth yield. Ann. Bot. 48, 275–290.

Moing, A., Escobar-Gutierrez, A., Gaudillère, J.P., 1994. Modeling carbon export out of mature peach leaves. Plant Physiol. 106, 591–600.

Möllney, M., Wiechert, W., Kownatzki, D., de Graaf, AA., 1999. Bidirectional reaction steps in metabolic networks: IV. Optimal design of isotopomer labeling experiments. Biotechnol. Bioeng. 66 (2), 86–103.

Neuhaus, H., Hausler, R., Sonnewald, U., 2005. No need to shift the paradigm on the metabolic pathway to transitory starch in leaves. Trends Plant Sci. 10, 154–156.

Nolte, K.D., Koch, K.E., 1993. Companion-cell specific localization of sucrose synthase in zones of phloem loading and unloading. Plant Physiol. 101, 899–905.

Patron, N.J., Greber, B., Fahy, B.F., Laurie, D.A., Parker, M.L., Denyer, K., 2004. The lys5 mutations of barley reveal the nature and importance of plastidial ADP-Glc transporters for starch synthesis in cereal endosperm. Plant Physiol. 135, 2088–2097.

Pelleschi, S., Rocher, J.P., Prioul, J.L., 1997. Effect of water restriction on carbohydrate metabolism and photosynthesis in mature maize leaves. Plant Cell Environ. 20, 493–503.

Rontein, D., Dieuaide-Noubhani, M., Dufourc, E.J., Raymond, P., Rolin, D., 2002. The metabolic architecture of plant cells. Stability of central metabolism and flexibility of anabolic pathway during the growth cycle of tomato cells. J. Biol. Chem. 277, 43948–43960.

Roscher, A., Emsley, L., Raymond, P., Roby, C., 1998. Unidirectional steady state rates of central metabolism enzymes measured simultaneously in a living plant tissues. J. Biol. Chem. 273, 25053–25061.

Ruan, Y.L., Chourey, P.S., Delmer, D.P., Perez-Grau, L., 1997. The differential expression of sucrose synthase in relation to diverse patterns of carbon partitioning in developing cotton seed. Plant Physiol. 115, 375–385.

Saglio, P.H., Pradet, A., 1980. Soluble sugar, respiration, and energy charge during aging of excised maize root tips. Plant Physiol. 66, 516–519.

Salon, C., Raymond, P., Pradet, A., 1988. Quantification of carbon fluxes through the tricarboxylic acid cycle in early germinating lettuce embryos. J. Biol. Chem. 263, 12278–12287.

Shannon, J.C., Pien, F.M., Liu, K.C., 1996. Nucleotides and nucleotide sugars in developing maize endosperms. Synthesis of ADP-glucose in brittle-1. Plant Physiol. 110, 835–843.

Subbaiah, C., Palaniappan, A., Duncan, K., Rhoads, D., Huber, S., Sachs, M., 2006. Mitochondrial localization and putative signaling function of sucrose synthase in maize. J. Biol. Chem. 281, 15625–15635.

Thibault, J.F., 1979. Automatisation du dosage des substances pectiques par la méthode au méta-hydroxydiphenyl. Lebensm-Wiss. U. Technol. 12, 247–251.

Toyota, K., Tamura, M., Nakamura, Y., 2006. Expression profiling of starch metabolism-related plastidic translocator genes in rice. Planta 223, 248–257.

Trethewey, R.N., Riesmeier, J.W., Willmitzer, L., Stitt, M., Geigenberger, P., 1999. Tuber-specific expression of a yeast invertase and a bacterial glucokinase in potato leads to an activation of sucrose phosphate synthase and the creation of a sucrose futile cycle. Planta 208 (2), 227–238.

Turner, .L., Plaxton, W.C., 2003. Purification and characterization of pyrophosphate- and ATP-dependant phosphofructokinases from banana fruit. Planta 217, 113–121.

Wang, F., Sanz, A., Brenner, M.L., Smith, A., 1993. Sucrose synthase, starch accumulation, and tomato fruit sink strength. Plant Physiol. 101, 321–327.

Wiechert, W., de Graaf, A.A., 1997. Bidirectional reaction steps in metabolic networks: I. Modeling and simulation of carbon isotope labeling experiments. Biotechnol. Bioeng. 55 (1), 101–117.

Wiechert, W., Siefke, C., de Graaf, A.A., Marx, A., 1997. Bidirectional reaction steps in metabolic networks: II. Flux estimation and statistical analysis. Biotechnol. Bioeng. 55 (1), 118–135.

Wiechert, W., Mollney, M., Isermann, N., Wurzel, M., de Graaf, A.A., 1999. Bidirectional reaction steps in metabolic networks: III. Explicit solution and analysis of isotopomer labeling systems. Biotechnol. Bioeng. 66 (2), 69–85.

Wiechert, W., Möllney, M., Petersen, S., de Graaf, A.A., 2001. A universal framework for ^{13}C metabolic flux analysis. Metab. Eng. 3 (3), 265–283.

Xu, D.P., Sung, S.J.S., Loboda, T., Kormanik, P.P., Black, C.C., 1989. Characterization of sucrolysis via the uridine diphosphate and pyrophosphate-dependent sucrose synthase pathway. Plant Physiol. 90, 635–642.

Zrenner, R., Salanoubat, M., Willmitzer, L., Sonnewald, U., 1995. Evidence of the crucial role of sucrose synthase for sink strength using transgenic potato plants (*Solanum tuberosum* L.). Plant J. 7, 97–107.